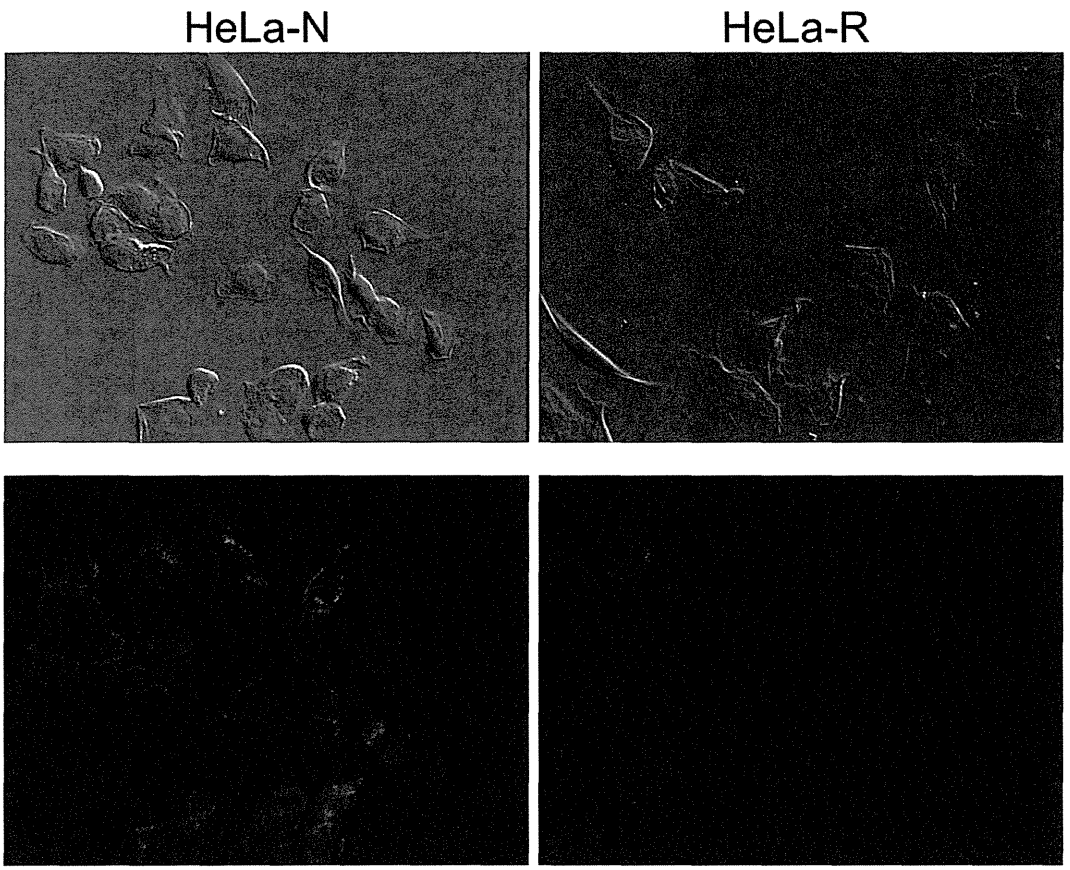

Figure 5. Immunofluorescent detection of the virus binding. The photos show the virus binding to the cell surface molecule(s) of each cell line. The cells fixed by 10% formalin were incubated with virus (MOI of 100). Then the viruses binding to the cell surface molecule(s) were detected by anti-SAFV-3 antiserum pre-absorbed by the homogenates of HeLa-R cells and Alexa Fluor 594-conjugated anti-rabbit IgG antibody. Left panels: HeLa-N cells, Right panels: HeLa-R cells. Upper and lower panels show Nomarski and fluorescent images, respectively. The viruses binding to cell surface of HeLa-R cells was significantly few, suggesting that the expression of receptor for SAFV infection is low in HeLa-R cells. Magnification: ×400.
doi:10.1371/journal.pone.0053194.g005

HeLa-R cells did not increase even at 14 days post-treatment (data not shown). On the other hand, CPE on PSAF/HeLa-R cells clearly increased within 12 days by the change of the serum for cell maintenance from CS to FCS (Fig. 4A). Furthermore, virus antigen was detected in most of PSAF/HeLa-R cells cultured with FCS, although it was detected in a part of PSAF/HeLa-R cells cultured with CS (Fig. 4B). However, PSAF/HeLa-R cells maintained with FCS did not die out for the additional 2 weeks.

Table 2. The titers of viruses produced from HeLa-N and HeLa-R transfected with viral recombinant transcripts.

		Viral titers (pfu/mL)	
		Means	**S.D.**
HeLa-N	Sup	93.3	58.0
	Cell	913.3	96.1
HeLa-R	Sup	373.3	89.6
	Cell	1106.7	436.6

Viruses were harvested at 16 hours post-transfection. Titers shown are the means and standard deviations (S.D.) in three independent experiments.
doi:10.1371/journal.pone.0053194.t002

Virus Binding Assay

In order to clarify whether SAFV persistence is dependent on the receptor expression, the virus binding assay was performed (Fig. 5). The viruses bound to the cell surface molecule(s) of HeLa-N cells were significantly numerous compared with those of HeLa-R cells.

Viral Titration After the Transfection of SAFV Recombinant Transcripts

To obtain further evidence that receptor densities are the (main) cause of cell-type differences, viral titers were determined after transfection of SAFV recombinant transcripts in both cell lines (Table 2). The titers of cell-free and cell-associated SAFV produced from HeLa-N cells at 16 hours post-transfection were 9.3×10^{1} pfu/ml and 9.1×10^{2} pfu/ml, respectively. On the other hand, the titers of cell-free and cell-associated SAFV produced from HeLa-R cells at 16 hours post-transfection were 3.7×10^{2} pfu/ml and 1.1×10^{3} pfu/ml, respectively. The titers of SAFV produced from both cell lines after RNA transfection were equivalent level.

Discussion

SAFV was identified as a novel human cardiovirus in 2007 [1] although cardioviruses have been thought to mainly infect rodents.

Several reports suggest that the virus may have diverse potential pathogenicity (e.g. respiratory illness, gastrointestinal illness, neurological diseases and/or type I diabetes) [7]. However, it is not clear that SAFV is the pathogen causing those clinical presentations. Since the potential persistence of SAFV is an important issue as described in "Introduction", in the present study, the possibilities of the persistent infection of SAFV were analyzed.

We first investigated on the differences of the growth of SAFV-3 in two HeLa cell lines, HeLa-N and HeLa-R, which are derived from different laboratories. As shown in Fig. 1A, the growth kinetics of SAFV-3 was significantly different in these two subtypes of cells although the growth kinetics of DA strain of TMEV was similar in both cell lines (Fig. 1B). STR analysis demonstrated that HeLa-N and HeLa-R cells were genomically identical (Fig. 2). Therefore, it was thought that the maintenance in a different condition has changed the phenotype(s) of these cells, which affect the SAFV growth but not affect the TMEV growth. We next observed the CPE after SAFV infection on HeLa-N and HeLa-R cultured in several conditions (Table 1). CPE by SAFV-3 infection on HeLa-N cells was severer than that on HeLa-R cells in the same conditions. Furthermore, the CPE by SAFV-3 infection on HeLa-N cells cultured with FCS are severer than that on HeLa-N cells pre-cultured with CS for 2 weeks. However, HeLa-N cells incubated with 1% CS after infection (without 2-week pre-culture with 10% CS) showed the CPE almost similar to that observed in HeLa-N cells incubated with 1% FCS after infection (data not shown). In addition, the neutralization test demonstrated that CS does not inhibit the virus infection. These data suggest that the inhibitor(s) against SAFV-3 were not contained in CS. On the other hand, HeLa-R cells incubated with 1% FCS after infection (without pre-culture with 10% FCS) also showed the CPE almost similar to that observed in HeLa-R cells incubated with 1% CS after infection (data not shown). In addition, even 2-week pre-culture with FCS cannot induce CPE in HeLa-R cells as severely as in HeLa-N cells, suggesting that the appearance of CPE may not be due to a direct enhancement of virus growth by the contents of FCS. Therefore, the severity of CPE is thought to depend on the unknown host factors(s) induced by the long-period culture with FCS.

Milder CPE of HeLa-R cells cultured with CS led us to attempt to establish the persistent infection of SAFV-3 on HeLa-R cells cultured with CS. Surviving cells after infection could be easily sub-cultured in fresh MEM with 10% CS although HeLa-N cells died out. Survived sub-cultured cells were designated "PSAF/HeLa-R". Persistent infection of SAFV-3 in PSAF/HeLa-R was demonstrated by Western blotting (Fig. 3) and plaque assay. The type of viral persistence of PDAJ774 cells, which is a murine macrophage-like cell line J774 persistently infected with TMEV-DA [15], belongs to the chronic focal infection according to the classification by Boldogh et al. [16]. In the case of PDAJ774 cells, the chronic focal infection was collapsed by the treatment with anti-mouse IFN-β antibody (80 U/ml/48 h) within 8 days [15], suggesting that it depends on type I IFN response of the host cells. However, the condition of PSAF/HeLa-R cells was not changed by the treatment with anti-human IFN-α antibody (1 μg/ml/48 h) or anti-human IFN-β antibody (120 U/ml/48 h) even at 14 days post-treatment. In addition, the number of virus antigen positive cells clearly increased in the culture with FCS for 12 days (Fig. 4B). These results suggest that the persistent infection of SAFV-3 in PSAF/HeLa-R cells does not depend on type I IFN response of host cells unlike the case of PDAJ774. In coxsackievirus, viral persistence is influenced by the cell cycle status [17] and/or the receptor expression [18]. Since the growth of HeLa-N and HeLa-R cells is similarly well in the medium supplemented with FCS or CS, the effects of the culture with FCS or CS on the cell cycle status is hardly analyzed. Therefore, we tried to compare the receptor expression of HeLa-N and HeLa-R cells by the virus binding assay, although the receptor for SAFV infection is not identified. Interestingly, the virus binding assay demonstrated that the expression of the virus binding molecule(s) (apparently SAFV receptor) on cell surface is significantly higher in HeLa-N cells cultured with FCS (Fig. 5). Additionally, to confirm the influence of the expression of receptor(s) to SAFV-3, cells were infected with SAFV-3 at a low MOI (0.5 pfu per cell) (Fig. S2). The viral antigen positive cells were significantly fewer in HeLa-R cells, suggesting that the efficiency of SAFV-3 infection in HeLa-R cells is low due to the low level expression of SAFV receptor(s). To further clarify this issue, viral titers after the transfection of the SAFV recombinant transcripts were determined in HeLa-N and HeLa-R cells. The results demonstrated that the (main) cause of cell-type differences is an entry suppression (apparently due to receptor densities), not a translation or replication block, since the both cell lines gave equivalent titers. These data suggested that SAFV persistence may depend on the receptor densities like the case of coxsackievirus [18]. The identification of the receptor(s) for SAFV infection will provide more critical evidence.

In conclusion, the present study demonstrated that SAFV is able to persist in human-derived cell line, HeLa cells. It brings up the possibility that SAFV may cause a persistent infection in humans as well as TMEV (the related virus) persists in mice. Furthermore, it was suggested that SAFV persistence may be influenced by the receptor expression of the host cells. The present findings of the *in vitro* SAFV-3 persistence will be helpful for further studies on the SAFV pathogenicity.

Supporting Information

Figure S1 Diagram showing the culture conditions for HeLa-N or HeLa-R cells. The closed and opened triangles represent the time point of the change of serum and the virus infection, respectively.
(TIF)

Figure S2 Immunofluorescent staining of the cells infected with SAFV-3 at a low MOI. Left panels show HeLa-N cells at 24 hours p.i. of SAFV-3 (MOI of 0.5), Right panels show HeLa-R cells at 36 hours p.i. of SAFV-3 (MOI of 0.5). Upper and lower panels show Nomarski and fluorescent images, respectively. Viral antigen was detected by anti-SAFV-3 antiserum pre-absorbed by the homogenates of HeLa-R cells and Alexa Fluor 594-conjugated anti-rabbit IgG antibody. Magnification: ×400.
(TIF)

Acknowledgments

We thank Dr. Nishikawa for his helpful suggestions and Ms. Saito for her excellent technical assistance.

Author Contributions

Conceived and designed the experiments: T. Himeda. Performed the experiments: T. Himeda. Analyzed the data: T. Himeda TO YM YO. Contributed reagents/materials/analysis tools: T. Hosomi. Wrote the paper: T. Himeda YO.

References

1. Jones MS, Lukashov VV, Ganac RD, Schnurr DP (2007) Discovery of a novel human picornavirus in a stool sample from a pediatric patient presenting with fever of unknown origin. J Clin Microbiol 45: 2144–2150.
2. Abed Y, Boivin G (2008) New Saffold cardioviruses in 3 children, Canada. Emerging Infectious Disease 14: 834–836.
3. Blinkova O, Kapoor A, Victoria J, Jones M, Wolfe N, et al. (2009) Cardioviruses are genetically diverse and cause common enteric infections in South Asian children. J Virol 83: 4631–4641.
4. Blinkova O, Rosario K, Li L, Kapoor A, Slikas B, et al. (2009) Frequent detection of highly diverse variants of cardiovirus, cosavirus, bocavirus, and circovirus in sewage samples collected in the United States. J Clin Microbiol 47: 3507–3513.
5. Zoll J, Erkens Hulshof S, Lanke K, Verduyn Lunel F, Melchers WJ, et al. (2009) Saffold virus, a human Theiler's-like cardiovirus, is ubiquitous and causes infection early in life. PLoS Pathog 5: e1000416.
6. Picornaviridae.com website. Available: http://www.picornaviridae.com/cardiovirus/theilovirus/safv.htm. Accessed 2012 Dec 6.
7. Himeda T, Ohara Y (2012) Saffold virus, a novel human cardiovirus with unknown pathogenicity. J Virol 86: 1292–1296.
8. Nielsen AC, Böttiger B, Banner J, Hoffmann T, Nielsen LP (2012) Serious invasive Saffold virus infections in children, 2009. Emerg Infect Dis. 18: 7–12.
9. Hertzler S, Liang Z, Treso B, Lipton HL (2011) Adaptation of Saffold virus 2 for high-titer growth in mammalian cells. J Virol 85: 7411–7418.
10. Sorgeloos F, van Kuppeveld F, Michiels T (2010) Saffold virus infection of the mouse. Abstr. Europic 2010, abstr. F-17, p. 104.
11. Himeda T, Ohara Y (2011) Roles of two non-structural viral proteins in virus-induced demyelination. Clin Exp Neuroimmunol. 2: 49–58.
12. Yoshitake Y, Nishikawa K (1992) Distribution of fibroblast growth factors in cultured tumor cells and their transplants. In Vitro Cell Dev Biol. 28A: 419–428.
13. Himeda T, Hosomi T, Asif N, Shimizu H, Okuwa T, et al. (2011) The preparation of an infectious full-length cDNA clone of Saffold virus. Virol J 8: 110.
14. Masters JR, Thomson JA, Daly-Burns B, Reid YA, Dirks WG, et al. (2001) Short tandem repeat profiling provides an international reference standard for human cell lines. Proc Natl Acad Sci U S A. 98: 8012–8017.
15. Himeda T, Okuwa T, Muraki Y, Ohara Y (2010) Cytokine/chemokine profile in J774 macrophage cells persistently infected with DA strain of Theiler's murine encephalomyelitis virus (TMEV). J Neurovirol 216: 219–229.
16. Boldogh I, Albrecht T, Porter DD (1996) Persistent viral infections. In Medical microbiology, 4th ed. Baron S (ed). Galveston, TX: The University of Texas Medical Branch at Galveston.
17. Feuer R, Mena I, Pagarigan R, Slifka MK, Whitton JL (2002) Cell cycle status affects coxsackievirus replication, persistence, and reactivation in vitro. J Virol 76: 4430–4440.
18. Pinkert S, Klingel K, Lindig V, Dörner A, Zeichhardt H, et al. (2011) Virus-host coevolution in a persistently coxsackievirus B3-infected cardiomyocyte cell line. J Virol 85: 13409–13419.

Vol. 29, No. 2, 2013 化学療法の領域

特集 ワクチン対策の現状と課題

3．ポリオワクチン

Poliovirus vaccine

中野 貴司*

ポリオ予防のワクチンは経口生ポリオワクチン（OPV）と不活化ポリオワクチン（IPV）がともに1950年代に開発された。OPVは血中中和抗体とともに腸管局所免疫も付与できる素晴らしい効果をもつワクチンであるが，頻度は低いものの，弱毒ワクチン株の神経病原性復帰によりワクチン関連性麻痺（VAPP）という副反応が起こる。一方，IPVではVAPPは起こらない。IPVは腸管局所免疫への期待は薄いがOPVに匹敵する免疫原性があり，同様の有効性が期待できる。現代はより安全なワクチンが待望され，OPVからIPVへの転換が行われている。わが国は海外に10年以上の遅れをとったが，最近2種類のIPVが導入された。世界で長年の経験のある単独IPVと，弱毒セービン株由来IPVを含有する四種混合ワクチン（DPT-IPV）である。これらについて概説する。

***Key Words*：ポリオ／VAPP／経口生ポリオワクチン／不活化ポリオワクチン／四種混合ワクチン**

I　ポリオと予防ワクチン

1．ワクチンの誕生

有史以来，人類を苦しめてきたポリオを予防できる2種類のワクチンが1950年代に開発された[1) 2)]。最初に華々しく登場したのはソーク博士（Jonas E. Salk）らが開発した不活化ポリオワクチン（inactivated poliovirus vaccine：**IPV**）であった。当時のアイゼンハワー米大統領はソークらの研究報告を支持し，全世界的にIPVを提供する用意があることを宣言した。

もうひとつのワクチンはセービン博士（Albert B. Sabin）らによる経口生ポリオワクチン（oral poliovirus vaccine：**OPV**）であった。その頃，世界は米国とソ連（ソビエト連邦・当時）の東西冷戦の時代であった。セービンは米国人であるがソ連でOPVの大規模な野外投与が行われ，素晴らしい有効性の報告がまとめられた。

2．わが国とポリオワクチン[1) 2)]

わが国は1960年に未曽有のポリオ大流行を経験し，年間の報告患者数は5,000名を越えた。ポリオによる麻痺は多くの場合，非可逆性であり，著明な筋萎縮と相まって後遺症につながる。患者好発年齢は小児であり，国民はこの病魔に怖れ慄いた。最流行期の夏を過ぎ，発生は一旦沈静化したが，次シーズンに備えるための手段，すなわち予防のためのワクチン導入が国全体を巻き込んで議論され，社会問題となった。

翌1961年初頭にはソークIPVの「希望接種」が実施されたが，全国から多数の申し込みがあり，輸入されたIPVの量では希望者全員に行き渡らなかった。やがて春を迎え，ふたたび流行が始まった。NHKテレビは4月から毎日，「ポリオ患者発生数即日集計」を全国放送した。流行は国内各地で発生し，国産IPVが検定不合格になったこともあり，IPVの供給はまったく不十分であった。

*川崎医科大学小児科 教授　Takashi Nakano

また，いつの時代にもある予防接種にはつきもののワクチン不信を煽るニュースであるが，IPVの「希望接種」を済ませた者からの発症も報告された。

わが国の母たちは，わが子をポリオから守りたい一心で，OPVの早期導入を求めて厚生省（当時）に押し寄せた。前年の勢いに劣らないポリオ患者増加の中で，世論の多くは海外で開発されて間もないOPVの緊急導入に積極的であった。そして1961年6月10日，羽田空港にOPVの原液がまず5万人分到着した。6月21日夕方，古井厚生大臣（当時）による「（OPV導入に関する）責任はすべて私にある」という談話とともに1,300万人分のOPV緊急輸入決定が発表された。6月26日，もっとも大きな流行が認められていた九州でOPVの「実験投与」が始まった。押し寄せるポリオ流行の波に押されるように，その後，OPVは各地で使われ，7月21日には全国の子どもたちを対象とした国内一斉投与が開始された。そして，ポリオ患者の発生が減少傾向に転じたのは500万人程度がOPV内服を済ませたと推計される7月末のことであった。

その後，わが国のポリオは完全に制圧された。やがて国産のOPVが製造されるようになり，定期接種ワクチンとして継続して実施され，ふたたびわが国でポリオが流行することはなかった。

Ⅱ　経口生ポリオワクチン（OPV）

OPVはワクチン成分として，1型，2型，3型のポリオウイルス弱毒株を含有する3価ワクチン

表1　OPVとIPVの比較

	OPV	IPV
接種後の腸管局所免疫	強力に獲得される（○）	獲得の期待は薄い（▲）
接種後の血清中和抗体	良好に上昇（○）	非常に良好に上昇（○）
便からのワクチン株ウイルス排泄	あり（▲）	なし（○）
ワクチン関連性麻痺（VAPP）の発生	数百万接種に一例有り（▲）	なし（○）
ワクチン由来株の伝播（cVDPV）	あり（▲）	なし（○）
集団免疫効果（Herd Immunity）	あり（○）	期待は薄い（▲）
高温暴露によるワクチンのダメージ	失活著明（▲）	失活する（▲）
投与法	経口で簡便（○）	注射が必要（▲）
他のワクチンとの混合製剤製造	期待薄い（▲）	可能（○）
価格	安価（○）	高価（▲）

長所に○，短所に▲を付した

OPVは血中中和抗体を獲得させるとともに腸管局所免疫も付与することができる，優れた効果をもつポリオ予防のためのワクチンである。経口投与できる簡便さや安価であるという長所もある。しかし，頻度は低いながらも弱毒ワクチン株の神経病原性復帰によりワクチン関連性麻痺（VAPP）という副反応が起こる。VAPPはOPV内服者が発症する以外に，糞便中に排泄されたウイルスが他人に伝播して起こることもある。IPVではVAPPは起こらない。

OPV：経口生ポリオワクチン，IPV：不活化ポリオワクチン

（文献3，4より）

IPV（inactivated poliovirus vaccine；不活化ポリオワクチン）

OPV（oral poliovirus vaccine；経口生ポリオワクチン）

で，開発者の名にちなんでセービン（Sabin）株と呼称される。自然感染と同じ経路で体内に投与され，腸管局所免疫を付与するとともに血清中和抗体も良好に上昇する。

接種により獲得される血中の中和抗体は約4週間でピークに達し，長年にわたって持続する。また，腸管局所免疫が獲得できることはOPVの大きな利点である。ポリオウイルス増殖の場である腸管の抵抗力が備わるため，ウイルスはそこに感染定着できない。OPVの一斉投与により短期間で流行を制御できる理由は，この点に負うところが大きく，OPVは集団免疫効果に優れたワクチンである。また，経口で簡便に投与できるということも長所である。1988年から始まった「世界ポリオ根絶計画（global polio eradication programme）」においてもOPVは世界各地でポリオを駆逐してきた。

その一方で，OPVにはワクチン株の神経毒性復帰と糞便中に排泄され伝播する性質に起因したワクチン関連性麻痺（vaccine-associated paralytic poliomyelitis：**VAPP**）などの短所がある[3)4)]（**表1**）。VAPPの頻度は決して高いわけではないが，OPVによる副反応であることは明らかであり，後遺症にもつながる。野生株ウイルスが駆逐され，長年ポリオの流行がない国や地域においてはOPVと同等の予防効果が期待され，より安全と考えられるワクチン，すなわちIPVへの切替えの必要性については多くの者の判断が一致する。OPVからIPVへの転換は副反応の確率論でも費用対効果の判断でもなく，より安全なワクチンへの転換の潮流である。

ただし，IPVはOPVと比べて高価であり，製造管理についても高度な水準が要求され，途上国の隅々まで普及させるには多くのハードルがある。

Ⅲ　不活化ポリオワクチン（IPV）

IPVもOPVと同様に，1型，2型，3型のポリオウイルスが混合されている。ただし，IPVの成分は感染性のない不活化されたポリオウイルスである。IPVがポリオを予防できる理論的根拠は，①ポリオウイルスに感染すると麻痺に先んじてウイルス血症が認められること，②血中に中和抗体が存在すれば麻痺発症を予防できることであ

表2　わが国の不活化ポリオワクチン（2012年12月時点）

	一般名	製造会社	販売名	承認	使用開始
単独IPV	不活化ポリオワクチン（ソークワクチン）	サノフィパスツール株式会社	イモバックスポリオ® 皮下注	2012年4月27日	2012年9月1日
四種混合（DPT-IPV）	沈降精製百日せきジフテリア破傷風不活化ポリオ（セービン株）混合ワクチン	阪大微研（大阪大学微生物病研究会）	テトラビック® 皮下注シリンジ	2012年7月27日	2012年11月1日
		化学及血清療法研究所	クアトロバック® 皮下注シリンジ		

わが国では，2012年9月に単独IPV，11月にDPT（ジフテリア・百日咳・破傷風）にIPVを混合した四種混合（DPT-IPV）ワクチンが導入された。

IPV：不活化ポリオワクチン

（薬剤添付文書の記載より筆者作成）

VAPP（vaccine-associated paralytic poliomyelitis；ワクチン関連性麻痺）

る[5)6)]。OPVと比較して腸管局所免疫を付与できる期待が薄いという弱点はあるが，VAPPの危険性がないことは大きな利点である（**表1**）。わが国では，2012年9月に単独IPV，11月に**DPT**（ジフテリア・百日咳・破傷風）にIPVを混合した四種混合（**DPT-IPV**）ワクチンが導入された（**表2**）。

表3　海外におけるIPVの免疫原性～接種後1カ月の時点における中和抗体価

IPV接種回数	接種時期	1型		2型		3型		実施研究数	接種対象者数
		陽性者の割合（%）	中和抗体GMT	陽性者の割合（%）	中和抗体GMT	陽性者の割合（%）	中和抗体GMT		
2	2カ月，4カ月	89～100	17～355	92～100	17～709	70～100	50～1,200	30	4,500
3	2カ月，4カ月，12～18カ月	94～100	495～2,629	98～100	1,518～6,637	97～100	1,256～4,332	10	2,000
3	2カ月，4カ月，6カ月	96～100	143～2,459	96～100	78～2,597	95～100	187～3,010	48	6,000
3	3カ月，4カ月，5カ月	85～100	110～475	98～100	92～944	86～100	89～1,244	8	500
3	2カ月，3カ月，4カ月	93～100	143～595	89～100	91～561	95～100	221～1,493	18	2,200

海外においてIPVの免疫原性を検討した研究結果の一覧である。2回接種で高い抗体陽転率が得られ，3回接種後は抗体価がさらに上昇する。それぞれ異なる研究として実施されたものであるため，単純に相互の数値比較はできない。

IPV：不活化ポリオワクチン，GMT：geometric mean titer（幾何平均抗体価）

（文献4，5より）

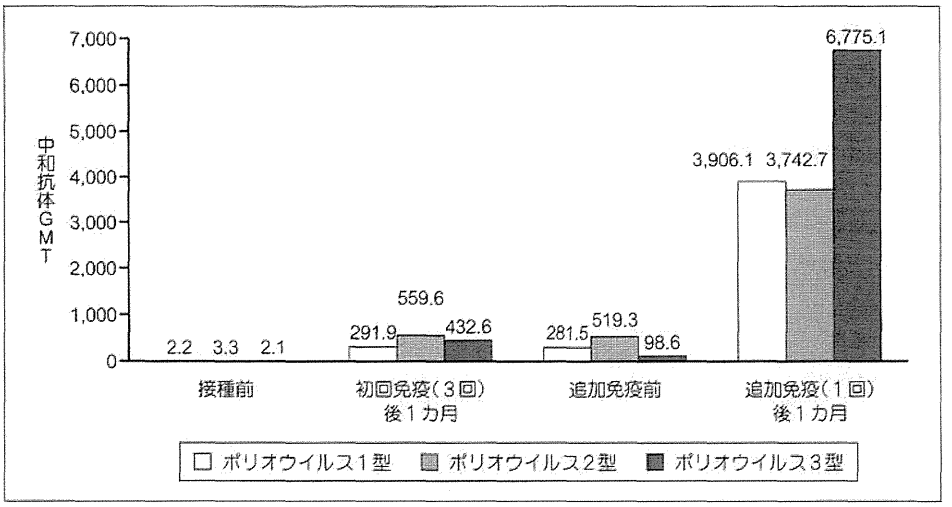

図1　イモバックスポリオ® 皮下注 国内第Ⅲ相臨床試験（免疫原性）

単独IPVの国内第Ⅲ相臨床試験における免疫原性の結果である。1型，2型，3型ポリオウイルスに対する中和抗体価は，初回免疫（3回接種）後にそれぞれ291.9，559.6，432.6倍，追加免疫（4回目接種）後にそれぞれ3,906.1，3,742.7，6,775.1倍と上昇し，いずれの型に対しても良好な免疫原性が確認された。

IPV：不活化ポリオワクチン　GMT：geometric mean titer（幾何平均抗体価）

（「イモバックスポリオ® 皮下注」総合製品情報概要より筆者作成）

DPT（ジフテリア・百日咳・破傷風）　　**DPT-IPV**（四種混合）

1．単独IPV

(1) 概　要

1950年代半ばにソークらが初めてIPVを開発した頃から，1型：Mahoney，2型：MEF-1，3型：Saukett株が使われ，現在も世界のほとんどの国でこの3種類の野生強毒株由来の不活化ウイルスが使用される。現在のIPVは開発当初の製剤と比べて，濃縮精製工程やD抗原定量法の導入により免疫原性の高いワクチンに改良されている。改良当初は強化不活化ポリオワクチン（enhanced potency IPV：**eIPV**）と呼ばれたが，今ではすべてのIPVがeIPVである。含有されるD抗原の量は，かつては1型20単位・2型2単位・3型4単位であったが，現在は1型40単位・2型8単位・3型32単位という組成である。開発当初のものより免疫原性が高くなったIPVはより高い予防効果を期待できると考えられている。規定回数を接種した場合，麻痺性ポリオを予防できる有効率は，ソークワクチンで80～90%，現在のIPVでは90%以上とされる[5]。

(2) 免疫原性

海外において検討された免疫原性の結果を**表3**に示した[4][5]。これらは単独IPV以外にDPTなどとの混合ワクチンを用いた成績も含んでいる。それぞれ異なる研究として実施されたものであるため相互の比較はできないが，2回接種で高い抗体陽転率が得られ，3回接種後は抗体がさらに上昇する。長期的な予防効果について中和抗体価で判定すると，欧米の定期接種スケジュールでIPVを4～5回接種した後は初回免疫から5～10年以

表4　イモバックスポリオ® 皮下注 国内第Ⅲ相臨床試験（接種回別の注射部位反応と全身反応）

	発現率（%）（発現例数/評価例数）			
	初回免疫			追加免疫
	1回目	2回目	3回目	
注射部位反応				
紅斑	51.4 (38/74)	51.4 (38/74)	47.3 (35/74)	52.1 (38/73)
腫脹	20.3 (15/74)	27.0 (20/74)	21.6 (16/74)	27.4 (20/73)
疼痛	2.7 (2/74)	1.4 (1/74)	5.4 (4/74)	8.1 (10/73)
発疹	0 (0/74)	0 (0/74)	1.4 (1/74)	0 (0/73)
全身反応				
易刺激性	17.6 (13/74)	16.2 (12/74)	14.9 (11/74)	21.9 (16/73)
傾眠状態	12.2 (9/74)	17.6 (13/74)	12.2 (9/74)	17.8 (13/73)
嘔吐	8.1 (6/74)	10.8 (8/74)	5.4 (4/74)	6.8 (5/73)
異常号泣	6.8 (5/74)	10.8 (8/74)	5.4 (4/74)	11.0 (8/73)
発熱（腋窩体温≧37.5℃）	5.4 (4/74)	5.4 (4/74)	4.1 (3/74)	21.9 (16/73)
食欲不振	6.8 (5/74)	6.8 (5/74)	1.4 (1/74)	17.8 (13/73)
下痢	0 (0/74)	2.7 (2/74)	0 (0/74)	4.1 (3/73)
けいれん	0 (0/74)	0 (0/74)	1.4 (1/74)	0 (0/73)

単独IPV接種後7日間の注射部位および全身の反応を観察した。接種後に偶発的に出現する事象の頻度も考慮すれば，安全性に関する大きな懸念事項は認めないと考えられる。

IPV：不活化ポリオワクチン

（「イモバックスポリオ® 皮下注」総合製品情報概要より）

eIPV (enhanced potency IPV；強化不活化ポリオワクチン)

上は免疫が保持されると考えられる[5]。

国内第Ⅲ相臨床試験は生後3～68カ月（生後3～8カ月を推奨）の健康小児74名を対象として単群（対照群を設定せず）で実施された。接種スケジュールは，初回接種として3～8週間隔でイモバックスポリオ® 皮下注0.5mLを3回接種し，その後，追加免疫として初回免疫終了後6～18カ月に単回接種して評価した。すなわち，DPTと同様の接種スケジュールである。3回目接種後のポリオウイルス1型，2型，3型に対する発症防御レベル（8倍）以上の中和抗体保有率はいずれも100%で，幾何平均抗体価（geometric mean titer：GMT）は1回目接種前では，1型，2型，3型それぞれ2.2，3.3，2.1倍であったが，3回目接種後ではそれぞれ291.9，559.6，432.6倍であり，いずれの型に対しても良好な免疫原性が確認された。そして4回目の追加免疫後には，1型，2型，3型それぞれ3906.1，3742.7，6775.1倍と，さらに大きく上昇した（**図1**）。

（3）安全性

安全性については，海外では長年広く用いられ，安全なワクチンと位置づけられている。接種部位の発赤：2%以内，硬結：数～10%，圧痛：10～30%などが報告されているが重篤な副反応は認められていない[5]。DPT，さらにはB型肝炎やHib（インフルエンザ菌b型）との混合ワクチ

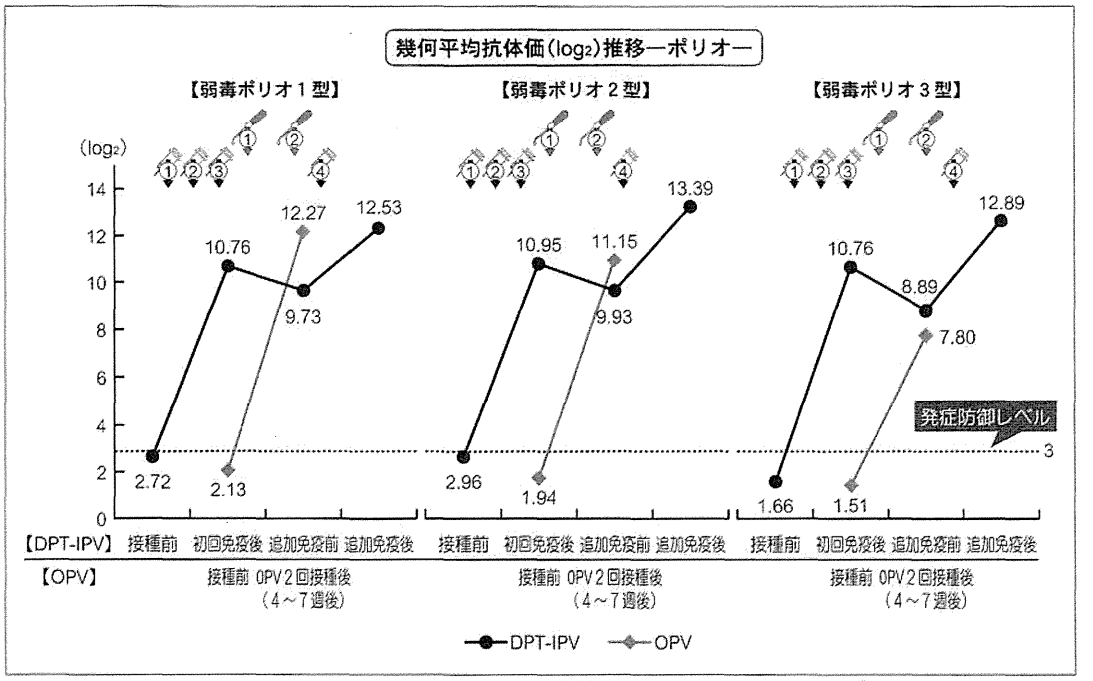

図2 DPT-IPV，OPV接種後のポリオ中和抗体価推移（テトラビック® 第Ⅲ相臨床試験）

DPT-IPV（テトラビック®）の国内第Ⅲ相臨床試験における免疫原性の結果である。1型，2型，3型ポリオウイルスに対する中和抗体価は，初回免疫（3回接種）後にそれぞれ$2^{10.76}$，$2^{10.95}$，$2^{10.76}$倍，追加免疫（4回目接種）後にそれぞれ$2^{12.53}$，$2^{13.39}$，$2^{12.89}$倍と上昇した。いずれの型のポリオウイルスに対しても良好な免疫原性が確認され，対照群として実施したOPV 2回接種と比べて同等あるいはそれ以上の免疫原性を示した。

DPT-IPV：四種混合，OPV：経口生ポリオワクチン

（「テトラビック® 皮下注シリンジ」審査報告書より筆者作成）

GMT（geometric mean titer；幾何平均抗体価）　Hib（インフルエンザ菌b型）

ンを用いた場合でもIPVの副反応が増強することはない。ただし，本剤との因果関係は明確ではないが，ギラン・バレー症候群，急性散在性脳脊髄炎の報告はある。

国内第Ⅲ相臨床試験では本剤接種後7日間の注射部位および全身の反応を観察した。接種回別の発現率を**表4**に示すが，問題となる重篤な副反応の報告はなく，接種後に偶発的に出現する事象の頻度も考慮すれば，現状で安全性に関する大きな懸念事項は認めないと考えられる。

2．四種混合ワクチン（DPT-IPV）

（1）概　要

わが国で開発された四種混合（DPT-IPV）ワクチンに含有されるIPVは弱毒セービン株由来の不活化ポリオワクチン（sabin-strain derived IPV：**sIPV**）である。OPVの成分である弱毒ポリオウイルスセービン株の1型，2型および3型をそれぞれVero細胞で培養し，濃縮・精製し，ホルマリン不活化後，3つの型を混合して日本ポリオ研究所で製造される。sIPVに含有されるD抗原の量は1型1.5単位・2型50単位・3型50単位という組成である。この3価混合不活化ポリオワクチン原液をDPTと混合して最終バルクを調整し，シリンジに充填したものが国内2社のDPT-IPVであり，チメロサールなど保存剤は含有していない。

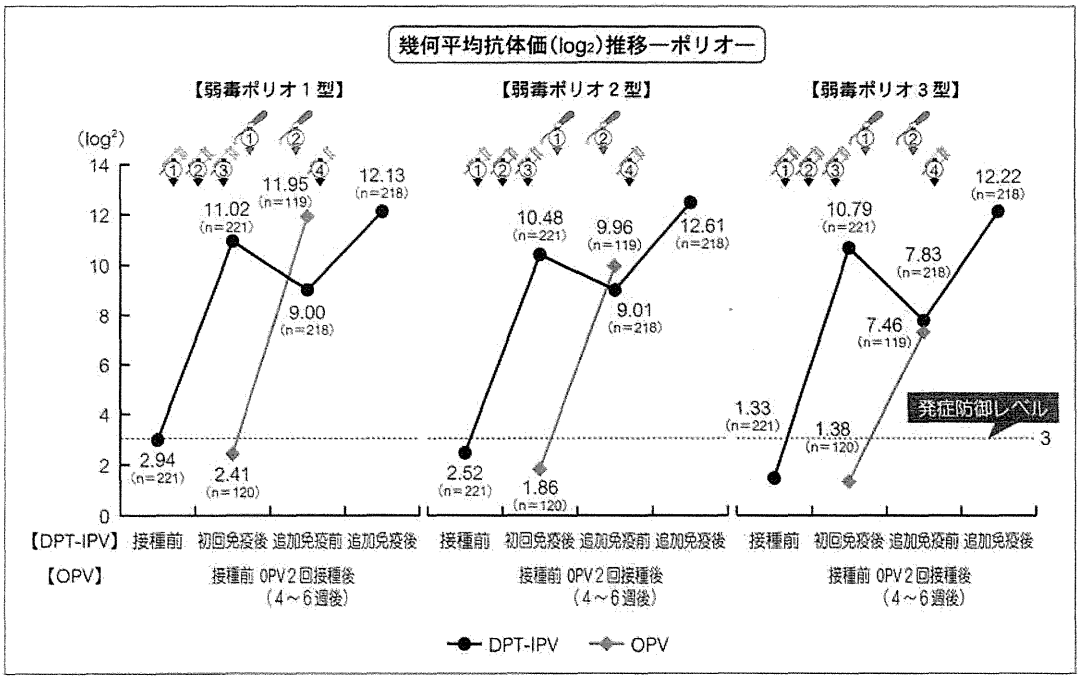

図3　DPT-IPV，OPV接種後のポリオ中和抗体価推移（クアトロバック® 第Ⅲ相臨床試験）

DPT-IPV（クアトロバック®）の国内第Ⅲ相臨床試験における免疫原性の結果である。1型，2型，3型ポリオウイルスに対する中和抗体価は，初回免疫（3回接種）後にそれぞれ$2^{11.02}$，$2^{10.48}$，$2^{10.79}$倍，追加免疫（4回目接種）後にそれぞれ$2^{12.13}$，$2^{12.61}$，$2^{12.22}$倍と上昇した。いずれの型のポリオウイルスに対しても良好な免疫原性が確認され，対照群として実施したOPV 2回接種と比べて同等あるいはそれ以上の免疫原性を示した。

DPT-IPV：四種混合，OPV：経口生ポリオワクチン

（「クアトロバック® 皮下注シリンジ」審査報告書より筆者作成）

sIPV (sabin-strain derived IPV；不活化ポリオワクチン)

DPT-IPV の接種月齢・回数・間隔は従来の DPT ワクチンのそれと同様である。IPV 導入に際しては近年過密になりつつある乳児期の予防接種スケジュールへの配慮も求められる。混合ワクチンや同時接種を活用して効率のよい免疫付与を心がけることが大切である。DPT-IPV は接種スケジュールへの負担を軽減しながら効率的な免疫獲得が可能となり，その有効な活用が期待されるワクチンである。今後さらに，Hib や B 型肝炎も含有する多価混合ワクチンの開発が望まれる。

(2) 免疫原性

DPT-IPV の国内第Ⅲ相臨床試験では２製剤(テトラビック® 皮下注シリンジ，クアトロバック® 皮下注シリンジ) とも DPT-IPV 接種群と対照群を設定し，対照群には二重盲検で DPT と OPV を接種した。したがって，ポリオ抗体価については OPV との比較，ジフテリア・百日咳・破傷風抗体価については DPT との比較が行われた。

初回免疫３回接種後のポリオウイルス１型，２型，３型に対する中和抗体保有率は２製剤とも 100%であった。接種前後におけるポリオ中和抗体価 GMT の推移は，３回目接種後は２製剤ともポリオウイルス１型，２型，３型に対して 1,000 倍を超える中和抗体価が獲得された。そして，４回目の追加免疫後には２製剤ともポリオウイルス１型，２型，３型に対して数 1,000 倍の中和抗体価へとさらに大きく上昇した (**図２，３**)。本結果は対照群として実施した OPV の免疫原性と比較して同等あるいはそれ以上の結果であった。単独 IPV とは別々の臨床試験として実施され，中和抗体価も野生強毒株と弱毒セービン株に対する抗体価をそれぞれ異なる系で測定しているため単純な相互の比較はできないが，世界で多くの経験のある単独 IPV に匹敵する良好な免疫原性が確認され

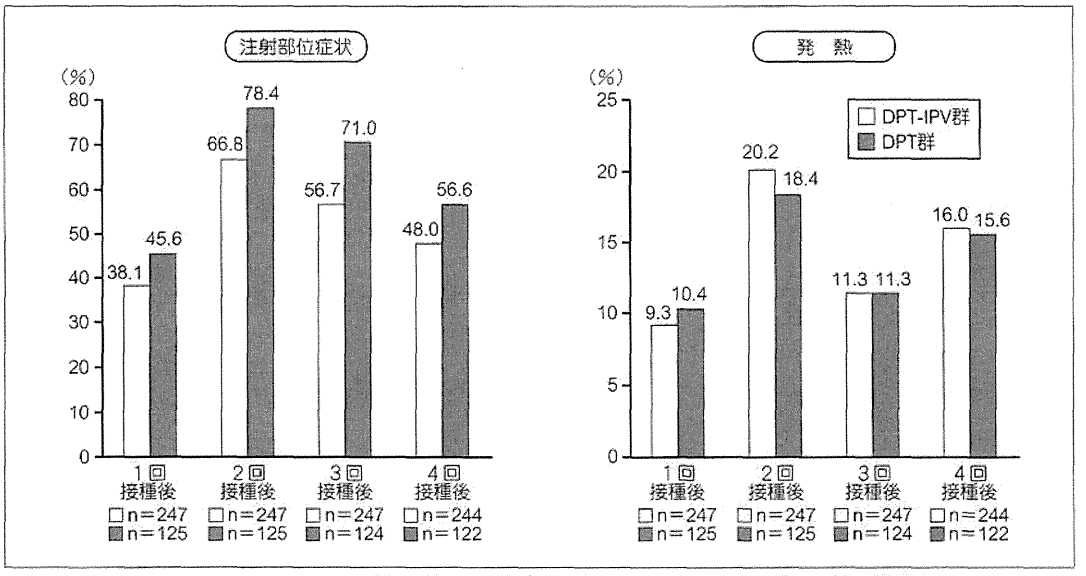

図４ DPT-IPV，DPT 接種後の副反応発現頻度 (テトラビック® 第Ⅲ相臨床試験)

DPT-IPV (テトラビック®) の国内第Ⅲ相臨床試験における DPT-IPV，DPT それぞれ接種後の副反応発現頻度である。DPT-IPV 群と対照群の DPT 接種後の注射部位反応および発熱の発現頻度を比較した結果，大きな差異はなかった。

DPT-IPV：四種混合，DPT：三種混合 (ジフテリア・百日咳・破傷風) ワクチン

(「テトラビック® 皮下注シリンジ」総合製品情報概要より筆者作成)

cIPV (conventional IPV)　　**VPD** (vaccine-preventable disease；ワクチン予防可能疾患)

たと考える。

ジフテリア・百日咳・破傷風抗体価については2製剤とも対照群におけるDPT接種後の免疫原性と比較して遜色はなかった。また，一部の症例ではHibワクチンとの同時接種が行われたが，同時接種により免疫原性が低下するということはなかった。

（3）安全性

テトラビック® 皮下注シリンジの国内第Ⅲ相臨床試験において1回目接種から4回目接種後4～7週までの期間に発現した有害事象の調査で観察されたおもな副反応は，注射部位の紅斑（74.5%），硬結（59.9%），腫脹（40.1%）や，発熱（38.9%）であった[7]。なお，本剤による重篤な副反応および臨床的に重大な問題となる有害事象は認められなかった。また，接種回数と注射部位の反応および発熱の発現率に相関は認められなかった。

クアトロバック® 皮下注シリンジの国内第Ⅲ相臨床試験で観察されたおもな副反応は，注射部位の紅斑（68.3%），硬結（52.0%），腫脹（31.2%）や，発熱（46.6%）であった[8]。

DPT-IPV接種群と対照群でのDPT接種後の注射部位反応および発熱の発現頻度を比較した結果，大きな差異はなかった。テトラビック® 皮下注シリンジの成績を**図4**に示すが，クアトロバック® 皮下注シリンジでも同様の結果であった。またDPTと比べて，注射部位反応や発熱などの全身症状に関して，程度の強い症状（局所反応が強い，発熱が高熱）の発現頻度もDPT-IPVで高くはなかった。すなわち，2つのDPT-IPV製剤は現行のDPTと同程度の副反応で，乳児でも安心して使えるワクチンと考えられた。

（4）sIPVの意義づけ

sIPVは世界に先駆けてわが国で承認されたが，ポリオ根絶計画の進展とも相まって製造施設の安全管理やバイオセーフティの観点からも注目され，欧州や中国など海外でも開発が進められている。世界で長年の経験がある野生株由来のconventional IPV（**cIPV**）と，わが国で開発されたsIPV，それぞれが今後，果たしていく役割にも注目が集まる。

Ⅳ 結 語

何よりも忘れてならないことは「ポリオは代表的なワクチン予防可能疾患（vaccine-preventable disease：**VPD**）」であり，ワクチンの普及に勝る制御法は存在しない。ソークとセービンが開発したワクチンは人類にはかり知れない恩恵を授けてくれた。これからも高い接種率を維持して，子どもたちを，そして人類をポリオから守っていくことが私たちの責務である。

文 献

1) 中野貴司：序（ミニ特集：不活化ポリオワクチン）．小児科臨床 **65**：2277-2280，2012.
2) 中野貴司：ポリオとポリオワクチン．化学療法の領域 **28**（8）：1751-1753，2012.
3) 中野貴司：ポリオウイルス．日常診療に役立つ小児感染症マニュアル2012．日本小児感染症学会編．東京医学社，東京．p482-489，2012.
4) 中野貴司：ポリオワクチン～生と不活化どちらがよいか．小児科診療 **75**：624-630，2012.
5) Plotkin SA, Vidor E：Poliovirus vaccine- inactivated. Vaccines. Plotkin SA, et al ed（5th ed）. Saunders，Philadelphia. p605-629，2008.
6) Sutter RW, Kew OM, Cochi SL：Poliovirus vaccine- live. Vaccines. Plotkin SA, et al ed（5th ed）. Saunders，Philadelphia. p631-685，2008.
7) 小川博暢，石川豊数：不活化ポリオワクチンの有効性と安全性（2）－沈降精製百日せきジフテリア破傷風不活化ポリオ（セービン株）混合ワクチン（テトラビック® 皮下注シリンジ）－（ミニ特集：不活化ポリオワクチン）．小児科臨床 **65**：2297-2306，2012.
8) 塩先巧一，城野洋一郎：不活化ポリオワクチンの有効性と安全性（3）－沈降精製百日せきジフテリア破傷風不活化ポリオ（セービン株）混合ワクチン（クアトロバック® 皮下注シリンジ）－（ミニ特集：不活化ポリオワクチン）．小児科臨床 **65**：2307-2317，2012.

JVI
Journals.ASM.org

The Association of Recombination Events in the Founding and Emergence of Subgenogroup Evolutionary Lineages of Human Enterovirus 71

E. C. McWilliam Leitch,[a] M. Cabrerizo,[b] J. Cardosa,[c] H. Harvala,[d] O. E. Ivanova,[e] S. Koike,[f] A. C. M. Kroes,[g] A. Lukashev,[e] D. Perera,[b] M. Roivainen,[h] P. Susi,[i] G. Trallero,[b] D. J. Evans,[j] and P. Simmonds[a]

Centre for Infectious Diseases, University of Edinburgh, Summerhall, Edinburgh, United Kingdom[a]; Enterovirus Laboratory, National Centre for Microbiology, Carlos III Institute of Health, Majadahonda, Madrid, Spain[b]; Institute of Health and Community Medicine, University Sarawak Malaysia, Sarawak, Malaysia[c]; Specialist Virology Centre, Royal Infirmary of Edinburgh, Edinburgh, United Kingdom[d]; M.P. Chumakov Institute of Poliomyelitis and Viral Encephalitides, Moscow, Russia[e]; Tokyo Metropolitan Institute of Medical Science, Tokyo, Japan[f]; Department of Medical Microbiology, Leiden University Medical Centre, Leiden, The Netherlands[g]; Intestinal Viruses Unit, National Institute for Health and Welfare, Helsinki, Finland[h]; Department of Virology, University of Turku, Turku, Finland[i]; and Department of Biological Sciences, University of Warwick, Coventry, United Kingdom[j]

Enterovirus 71 (EV71) is responsible for frequent large-scale outbreaks of hand, foot, and mouth disease worldwide and represent a major etiological agent of severe, sometimes fatal neurological disease. EV71 variants have been classified into three genogroups (GgA, GgB, and GgC), and the latter two are further subdivided into subgenogroups B1 to B5 and C1 to C5. To investigate the dual roles of recombination and evolution in the epidemiology and transmission of EV71 worldwide, we performed a large-scale genetic analysis of isolates (n = 308) collected from 19 countries worldwide over a 40-year period. A series of recombination events occurred over this period, which have been identified through incongruities in sequence grouping between the VP1 and 3Dpol regions. Eleven 3Dpol clades were identified, each specific to EV71 and associated with specific subgenogroups but interspersed phylogenetically with clades of coxsackievirus A16 and other EV species A serotypes. The likelihood of recombination increased with VP1 sequence divergence; mean half-lives for EV71 recombinant forms (RFs) of 6 and 9 years for GgB and GgC overlapped with those observed for the EV-B serotypes, echovirus 9 (E9), E30, and E11, respectively (1.3 to 9.8 years). Furthermore, within genogroups, sporadic recombination events occurred, such as the linkage of two B4 variants to RF-W instead of RF-A and of two C4 variants to RF-H. Intriguingly, recombination events occurred as a founding event of most subgenogroups immediately preceding their lineage expansion and global emergence. The possibility that recombination contributed to their subsequent spread through improved fitness requires further biological and immunological characterization.

Enterovirus 71 (EV71) is one of the most frequently detected pathogenic human enteroviruses, responsible for large-scale epidemic occurrences of neurological disease throughout Southeast Asia (51, 58). EV71 contains a single-stranded, positive-sense RNA genome and is classified as a member of species A (EV-A) in the *Enterovirus* genus of the *Picornaviridae* family (60). As with other EV-A enteroviruses, EV71 is transmitted by the fecal-oral route and normally causes subclinical or relatively mild, self-limiting infections, such as hand, foot, and mouth disease (HFMD) (65). However, unlike other members of EV-A, EV71 infections are associated in a small proportion of subjects with a wide array of severe disease presentations, including aseptic meningitis, encephalitis, and acute flaccid paralysis (AFP) (reviewed in references 29 and 58). Severe and fatal EV71 infections are predominantly found in young children, with male patients outnumbering female patients (12, 52). There has been a substantial increase in the frequency and severity of EV71 epidemics in recent years, particularly in the Asian Pacific region (5, 13, 58, 65), prompting urgent, ongoing investigations of the virological and host factors contributing to the apparently increasing pathogenicity of the virus (5, 11, 58).

Considerable insights into the evolution and molecular epidemiology of circulating strains and genotypes of EV71 from many of the most-affected countries have been obtained through analysis of structural genome regions, principally VP1. EV71 has been classified into a total of three genogroups (Ggs), designated GgA to GgC (6), showing approximately 13 to 20% amino acid sequence divergence from each other in the VP1 region (6, 28) and estimated to have originated from a common ancestor as recently as 1941 (61). Several studies have investigated whether different genogroups or subgenogroups vary in their pathogenicity, which might then explain the variability in outcomes of EV71 infections in different decades and between continents. While whole-genome sequence comparisons of EV71 strains isolated from severe or fatal cases of EV71 infection showed no reproducible differences from those causing more mild infections (54, 57), specific associations of GgC2 variants with severe neurological disease and of B3 with HFMD or mild/inapparent infections were observed during an outbreak in Perth, Australia, in 1988, when both genogroups were cocirculating (35, 36). More recently, a greater likelihood of GgC5 to cause neurological complications than GgC4 was reported (44).

In the current study we genetically characterized a large num-

Received 19 August 2011 **Accepted** 21 December 2011
Published ahead of print 28 December 2011
Address correspondence to P. Simmonds, Peter.Simmonds@ed.ac.uk.
Supplemental material for this article may be found at http://jvi.asm.org/.

doi:10.1128/JVI.06065-11

TABLE 1 Sources and collection dates of survey specimens

Virus and country	Code	No. of isolates	Subgenogroup(s)	Yr(s) of isolation
EV71				
Croatia	HR	2	C4	2005
Finland	FI	16	C1, C2, C5	1994, 2000–2005, 2007–2009
Georgia	GE	1	C2	2007
Great Britain	GB	5	C2	2010
Iceland	IS	2	C1	2004
Japan	JP	62	B2, B4, B5, C1, C2, C4	1990, 1993, 1997–2010
Latvia	LV	1	C1	2003
Malaysia	MY	83	B3, B4, B5, C1	1997–1998, 2000, 2002, 2003, 2006, 2008
The Netherlands	NE	15	C1, C2	2007, 2010
Russia	RU	6	C1, C2	2000, 2001, 2007–2009
Spain	ES	7	C1, C2	1999, 2002, 2003, 2007
Total (n = 11)		200		1990, 1993–1994, 1998–2010
CVA16				
Finland	FI	10		2000, 2001, 2003, 2005, 2006, 2008–2010
Great Britain	GB	1		2009
Iceland	IS	2		2002, 2004
Japan	JP	1		2004
Latvia	LV	1		2007
The Netherlands	NL	4		2008
Russia	RU	5		2008–2010
Slovak Republic	SK	2		2004–2005
Spain	ES	11		2000, 2003, 2006, 2008
Total (n =9)		37		2000–2010

ber of EV71 strains, collected from South and East Asia, Australia, and Europe, in the VP1 region and a distal region of the genome (part of the 3D polymerase-encoding region [3Dpol]) for identification of recombination events. Recombination is a frequently documented phenomenon in picornaviruses and contributes to their evolutionary diversity as well as a means to acquire new phenotypic traits from acquisition of novel combination of structural and nonstructural genes and 5′-untranslated region (5′-UTR) sequences.

Recombination in picornaviruses was first observed between serotypes of poliovirus in vaccine recipients (8, 20, 39) and more recently in a wide range of human enteroviruses (1, 15, 16, 21, 31, 41, 43, 45, 48, 56), foot-and-mouth disease virus (FMDV), and teschoviruses (55) and, more recently, parechoviruses (3, 4). In each virus, recombination breakpoints concentrate in the 2A region, although further sites occur in P2 and P3 genes and in the 5′-UTR (1, 3, 16, 30, 33, 49, 67). In contrast, phylogenies of the more divergent capsid-encoding genes VP1, VP2, and VP3 are congruent with each other (and correspond to their serotypic classification) (31, 42, 49), leading to the idea that sequence diversification in structural gene regions is largely uncoupled from that of nonstructural genes (31, 32, 37, 55). The contribution of recombination to the evolution and molecular epidemiology of EV71 and its relationship to diversification of capsid-encoding genes is the focus of the current study.

The study used a large data set of newly acquired and published sequences for the VP1 (capsid) and 3Dpol (nonstructural) gene regions of EV71 and coxsackievirus A16 (CVA16). The identification of recombination events was assisted through the assignment of 3Dpol sequences of EV71 isolates to individual recombinant forms, as developed for the analysis of EV species B viruses (37, 38). The study provides convincing evidence for recombination events in the founding of most subgenogroup lineages over an evolutionary time scale comparable to that observed within EV-B serotypes. These analyses further our understanding of the molecular epidemiology of EV71 and its varied clinical manifestations.

MATERIALS AND METHODS

Samples. A total of 193 isolates from 11 countries collected between the years 1990 and 2010 (Table 1) were obtained from internationally distributed referral centers. The following convention was used to name isolates: two-letter country code and isolate number/two-letter city or region abbreviation/3Dpol clade/year of collection (e.g., MY40/Sw/A/06 for isolate number 40 referred from Sarawak in Malaysia, isolated in 2006, and belonging to the 3Dpol clade A [defined below]). Sequences obtained in the current study were supplemented with 5 previously unpublished sequences from Russia collected between 2000 and 2009 and with 110 published sequences of complete genomes from 10 countries that were collected between 1970 and 2009, including the EV71 prototype strain BrCr-CA-70. All sequences in the current study were obtained from laboratory-passaged virus stocks, as were the published complete genome sequences of EV71 and CVA16 incorporated in the analysis. This greatly reduced the likelihood of sampling mixed virus populations that might, for example, have originated from coinfections of the study subjects with different EV71 or CVA16 strains.

Amplification of VP1 and 3Dpol regions and nucleotide sequencing. RNA extraction and nested reverse transcription-PCRs (RT-PCRs) were performed as previously described but using newly designed enterovirus primers specific for EV71 and CVA16. These amplified a 1,055-bp region of the VP1 gene and a 759-bp region of the 3Dpol gene. Primers com-

prised the following: for VP1, OS (outer sense; position 2268 in the poliovirus type 3 sequence; K01392), CCN TGG ATH AGY AAC ACN CAY T; OAS (outer antisense; position 3604), GAR AAR CTR ACY GGR TAG TGY TTT CT; IS (inner sense; position 2332), TNA SNA TYT GGT AYC ARA CAN AYT; and IAS (inner antisense; position 3409), ACR TAD ATD GCN CCN GAY TGY TG. For 3Dpol, the primers included OS (position 5830), GSA CYA TGA TGT AYA AYT TYC CHA C; OAS (position 7045), GGN GTC ATD GTY ARN CCR TAY TCY TT; IS (position 6261), ATG AGY ATR GAR GAN GCN TGY TAY G; and IAS (position 7195), TCY TTN GTC CAD CGR ATR GAY TCR T. Amplicons were directly sequenced using BigDye (Applied Biosystems), and the inner sense or antisense primer and nucleotide sequences were aligned with the Simmonic sequence package, version 1.9 (56; http://www.virus-evolution.org/Software). Confirmatory repetitions of RT-PCRs and sequencing were performed for all isolates that showed incongruences in tree positions between the VP1 and 3Dpol regions, as described below.

Phylogenetic analysis. Bootstrapped maximum likelihood trees for VP1 and 3Dpol regions were generated using RAxML with the GTRGAMMA model (general time-reversible plus gamma distribution for rates over sites, with all model parameters estimated using RAxML) and 100 bootstraps (59). Regression analysis and investigation of geographical and temporal aspects of recombination were performed using maximum composite likelihood (MCL) distances (calculated by using MEGA) between sequences.

A Bayesian Markov chain Monte Carlo (MCMC) method implemented in the BEAST package, version 1.53 (18), was used to estimate temporal phylogenies and rates of evolution (19). Individual data sets prepared for BEAST analysis (corresponding to genogroups, subgenogroups, or 3Dpol clades used to define RFs) were checked for recombination using the program Genetic Algorithm Recombination Detection (GARD) or the single breakpoint (SBP) method for larger VP1 data sets (GgC and RF-W) in the Datamonkey package, which provides an interface to the HyPhy program (27, 47). Further testing was performed on each data set by using several algorithms implemented in the RDP package (RDP, GENCONV, MaxChi, Chimaera, SiScan, and 3Seq [34]).

For BEAST analysis we used constant population size as a prior, while for selected data sets other tree priors were used (exponential growth, Bayesian Skyline) to determine the effect priors on analysis outcomes. Two independent runs for each set were analyzed using the SRD06 model of substitution (53), with chain lengths of 50 million or 100 million and a relaxed molecular clock model that allows evolutionary rates to vary among lineages. All other parameters were optimized during the burn-in period. Output from BEAST was analyzed using the program TRACER (http://beast.bio.ed.ac.uk/Tracer), and the results of each duplicate were compared. RF succession dynamics were examined using a maximum clade credibility (MCC) tree visualized in FigTree following annotation in Tree-Annotator.

Nucleotide sequence accession numbers. All newly generated sequences obtained in this study were submitted to GenBank and were assigned the accession numbers HQ676156 to HQ676288 (VP1) and HQ676289 to HQ676487 (3Dpol).

RESULTS

Phylogeny of EV71 VP1 and 3Dpol genome regions. A total of 198 EV71 isolates from 11 countries and 37 CVA16 isolates (Table 1) were analyzed in the current study concurrently with the prototype sequence BrCr-CA-70 (U22521; designated US01/CA/Q/70 in this study) and 109 previously published full-genome sequences of EV71 and 8 of CVA16 (see Table S1 in the supplemental material). EV71 and CVA16 sequences were amplified and sequenced in the VP1 region between positions 2458 and 3345 (numbering based on BrCr-CA-70). All EV71 isolates analyzed in the current study clustered with other EV71 sequences to form a monophyletic group separate from other EV-A serotypes/types (data not shown). The isolates assembled into the previously designated genogroups B2 to B5, C1, C2, C4, and C5; those from Europe were exclusively GgC1, GgC2, GgC3, and GgC5 (see Fig. S1 in the supplemental material).

For recombination analysis, sequences from the 3′ end of the genome (within the 3Dpol coding region) were determined for each of the 198 isolates analyzed in VP1, and the data set was combined with available complete genome sequences of EV71 and CVA16 (see Fig. S1 in the supplemental material). Sequences in the 3Dpol region formed a series of bootstrap-supported clades; EV71 3Dpol clades comprised groups A, D, E, G, H, L, Q, T, V, W, and Y, while clades C, I, J, M, O, and S were identified among CVA16 sequences. Individual genogroups were associated with specific 3Dpol clades in the majority of cases.

Supporting these phylogenetic assignments, the pairwise distributions of sequence distances between variants in both VP1 and 3Dpol fell into a series of discontinuous ranges (see Fig. S2A in the supplemental material). For example, the minimum value in the VP1 distribution separating the second and third distributions of approximately 19% corresponds to the threshold value separating intra- from intergenogroup distances between GgA, GbB, and GgC (6) (see Fig. S2A). The lower threshold value (10 to 11%) corresponded to the previously designated subgenogroup boundaries (6). An analogous division of 3Dpol sequences into the 15 clades by phylogenetic analysis was similarly supported by their distribution of pairwise distances (see Fig. S2B). The low point in the distribution, 0.13, corresponded closely to the threshold value dividing distances between and within the phylogenetically defined clades.

3Dpol classification provides the means to identify and quantify recombination events within data sets through identification of incongruences between phylogenetically supported clades in different genome regions, as used in previous analyses of EV-B serotypes (37, 38). 3Dpol gene sequences of the 15 RFs of EV71 and CVA16 indeed imperfectly mapped onto the phylogeny of the VP1 region and revealed several phylogeny violations indicative of recombination (Fig. 1). By branch rotation to maximize tree branching orders and by ignoring any phylogenetic grouping without 70% or more bootstrap support, trees from the two regions revealed both branching order differences within EV71 (red dotted lines) as well as highly interspersed groupings of CVA16 sequences in the 3DPol tree (red sequence labels) that contrasted with the consistent outgroup position of CVA16 in the VP1 region (Fig. 1).

As specific examples, GgB3 grouped with B4 and B5 in VP1 but adopted a distinct tree position in 3Dpol closest to C4 and CVA16 variants. The branching order of GgA was similarly incongruent. Within genogroups, while the majority of sequences were associated with a specific 3Dpol group, such as C2 with W and C4 with L, individual variants within each showed phylogenetically distinct 3Dpol sequences similarly indicative of recombination. Each of the CVA16 groups identified as separate RFs originated through at least 6 further recombination events in their evolutionary histories. This analysis depicts the minimum number of recombination events required to resolve the phylogenies of the available sequences. The interspersed nature of other EV-A 3Dpol sequences in the phylogenetic tree (data not shown) entails a much large number of further recombination events over the longer period of EV species A evolution.

Sequence diversification in VP1 and 3Dpol regions. EV71

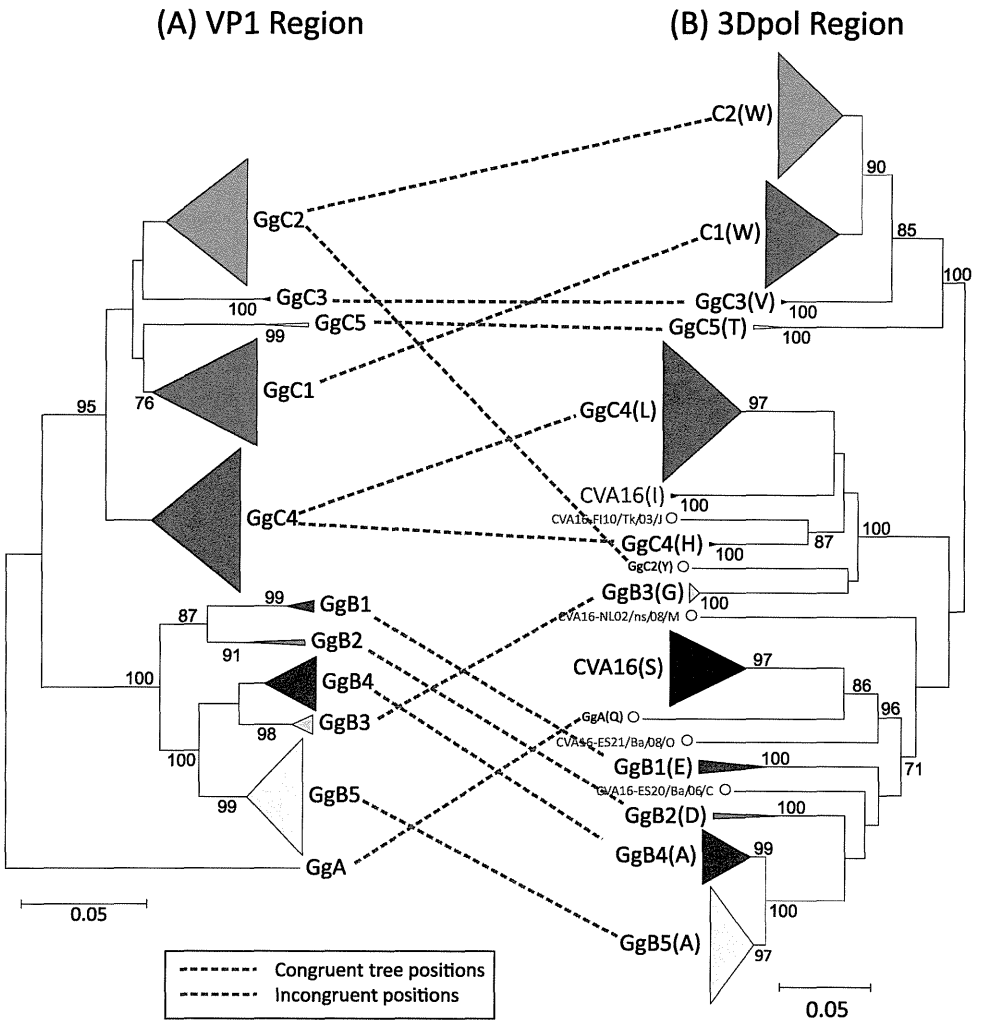

FIG 1 Phylogeny of VP1 and 3Dpol regions of EV71 for study subjects and those previously determined (listed in Table 1; see also Table S1 in the supplemental material). Clades were identified by bootstrap analysis (values of ≥70%) by maximum likelihood analysis as implemented using RAxML. The sizes of the triangles are proportional to the number of sequences within each clade (bootstrap resampling values are shown on branches). By branch rotation to maximize visual congruence of the two trees and the use of bootstrap values of ≥70% to define phylogenetic groupings, the minimum numbers of incongruent phylogeny relationships (depicted by red dotted lines) were determined (clades showing congruent branching orders labeled with blue dotted lines). The 3Dpol region includes available sequences from CVA16; these are labeled red, as their interspersed positions in 3Dpol are invariably incongruent with their outgroup position in VP1 (not included in the tree on the left).

VP1 variability was predominantly restricted to synonymous sites indicative of predominantly neutral sequence change. Using the data available on the collection dates of samples in a Bayesian MCMC method (BEAST [19]) with a relaxed molecular clock for substitution rate calculations, substitution rates, and times of most recent common ancestor (TMRCAs) of different genogroups and 3Dpol clades defining the largest RFs were calculated. Each data set was analyzed for internal recombination prior to BEAST analysis. GARD/SBP detected no recombination events in any data set, while detection of recombinant sequences using RDP-implemented methods was infrequent and inconsistent between methods (see Table S4 in the supplemental material). To investigate whether these possibly recombinant sequences influenced the validity of the MCMC analysis, one of the sequences in VP1 identified as recombinant by three methods (TW13) was excluded from the GgC data set, and CN01 was removed from the clade L 3Dpol sequence data set. Substitution rates and TMRCAs were compared with the full data sets (see Table S5 in the supplemental material). Effectively identical rates and dates were calculated for each comparison, indicating that intraclade recombination had no effect on the validity of the BEAST analysis.

The crude evolutionary rate of evolution for the whole data set of VP1 sequences was 7.2×10^{-3} substitutions/site/year (high-probability distribution [HPD] range, 6.2×10^{-3} to 8.3×10^{-3}) (Table 2), with a predicted TMRCA of all extant EV71 lineages of 80 years (HPD, 58 to 106 years). Analysis of individual genogroups within EV71, GgB, and GgC revealed comparable evolutionary rates of 6.2×10^{-3} substitutions/site/year (HPD range, 5.2×10^{-3} to 7.3×10^{-3}) for GgB and 5.0×10^{-3} substitutions/site/year (HPD range, 4.3×10^{-3} to 5.8×10^{-3}) for GgC and TMRCAs of 36 years (HPD, 35 to 38 years) and 34 years (HPD, 25 to 37 years), respectively. Similar substitution rates and more recent MRCAs (8 to 32 years) were observed among subgenogroups (Table 2).

TABLE 2 Rates of sequence change and TMRCAs by MCMC analysis

Genogroup and geographic set	Gg or RF	n^c	Divergence[a] Nucleotide VP1	Nucleotide 3Dpol	aa VP1	aa 3Dpol	Regression (R) VP1	Regression (R) 3Dpol	MCMC (BEAST)[b] Substitution rate (10^{-3})[d] VP1	Substitution rate (10^{-3})[d] 3Dpol	TMRCA[e] VP1	TMRCA[e] 3Dpol
Whole data set												
All	All	308	0.18	—	0.02	—	0.14	—	7.2 (6.2–8.3)	—	79.9 (58.2–105.5)	—
Europe	All	58	0.09	—	0.01	—	0.58	—	3.5 (1.9–5.1)	—	36.2 (19.4–58.1)	—
Asia	All	244	0.17	—	0.02	—	0.32	—	6.4 (5.2–7.8)	—	61.4 (45.8–79)	—
Individual genogroups												
All	GgB	108	0.07	—	0.01	—	0.94	—	6.2 (5.2–7.3)	—	35.9 (35–37.5)	—
All	GgC	199	0.13	—	0.02	—	0.77	—	5.0 (4.3–5.8)	—	30.7 (24.8–37.6)	—
Asia	GgC	137	0.11	—	0.01	—	0.77	—	5.4 (4.5–6.2)	—	27.4 (23.6–31.7)	—
Individual subgenogroups												
All	GgB4	28	0.03	—	0.01	—	0.7	—	6.8 (2.2–13)	—	8.3 (5.4–12.4)	—
All	GgB5	60	0.02	—	0.00	—	0.88	—	7.3 (4.6–10.4)	—	9.1 (8–10.6)	—
All	GgC1	55	0.05	—	0.01	—	0.86	—	3.2 (2.1–4.3)	—	31.2 (22.9–41.1)	—
All	GgC2	65	0.05	—	0.01	—	0.75	—	4.7 (3.1–6.2)	—	21.0 (15.4–28.8)	—
All	GgC4	74	0.04	—	0.01	—	0.75	—	6.0 (4.6–7.4)	—	15.4 (12.8–18.4)	—
Individual RF groups												
All	RF-A	88	0.05	0.06	0.01	0.01	0.92	0.95	6.4 (4.8–8.1)	6.7 (5.3–8.3)	13.3 (11.7–15.1)	13.9 (12.3–15.6)
All	RF-W	119	0.10	0.09	0.01	0.02	0.35	0.76	5.1 (3.8–6.5)	4.3 (2.7–5.9)	30.5 (23.3–38.9)	34.9 (24.5–47.9)
Asia	RF-W	61	0.10	0.09	0.01	0.02	0.64	0.75	5.2 (4.1–6.3)	5.7 (4.2–7.5)	26.1 (22.5–29.7)	24.5 (20.4–28.3)
Europe	RF-W	55	0.08	0.08	0.01	0.01	0.59	0.57	3.7 (2.2–5.4)	1.1 (0.4–1.9)	30.4 (17–47.3)	85.1 (28.8–161.3)
All	RF-L	72	0.04	0.04	0.01	0.01	0.85	0.89	5.9 (4.6–7.2)	5.4 (4.0–6.8)	15.5 (12.9–18.6)	18.8 (13.5–25.3)

[a] Mean pairwise P distances. —, values were not calculated for the 3Dpol region for groups in which 3Dpol sequences were not monophyletic. aa, amino acids.
[b] The mean value is based on two independent analyses; substitution rates and TMRCAs were not calculated for groups where 3Dpol sequences were not monophyletic.
[c] The number of sequences analyzed in each set.
[d] Frequency of substitutions per site per year (with HPD range shown in parentheses).
[e] Time before the present of the most recent common ancestor (in years).

For the three larger RF groups (RF-A, RF-L, and RF-W), remarkably similar substitution rates for individual clades were determined in the 3Dpol region (Table 2). For example, the substitution rate for RF-A was 6.4×10^{-3} substitutions/site/year (HPD range, 4.8×10^{-3} to 8.1×10^{-3}) in the VP1 region and 6.7×10^{-3} substitutions/site/year (HPD range, 5.3×10^{-3} to 8.3×10^{-3}) in the 3Dpol region. Furthermore, both genome regions analyzed provided consistent estimates for the TMRCAs of each individual RF group analyzed; using again the example of RF-A, TMRCAs of 13.3 years (HPD, 11.7 to 15.1) and 13.9 years (HPD range, 12.3 to 15.6) for VP1 and 3Dpol, respectively, were observed. These data provided robust estimates for the dates of the recombination events that created each RF.

To determine whether the prior on the tree in the BEAST analysis influenced estimates of substitution rate or TMRCA, analyses were repeated using exponential growth and Bayesian Skyline analyses for the larger data sets (GgB and GgC in VP1 and RF-L and RF-W in 3Dpol) (see Table S3 in the supplemental material). Each prior produced extremely similar values for substitution rate and TMRCA in each data set. Sequence relationships between dated samples collected over a wide temporal range primarily informed these calculations rather than tree prior.

The similar dynamics of sequence drift between VP1 and 3Dpol regions and the disruptive effect of recombination were apparent through comparison of pairwise distances in the two genome regions of the better-represented subgenogroups (Fig. 2; examples of B4 and C1 are shown). Discontinuities in the distributions of pairwise distances supported the hypothesis of widespread recombination during EV71 evolution. Within-genogroup GgB4 and GgC1 comparisons showed an approximate straight line correlation between VP1 and 3Dpol divergence (dark blue points), with a positive gradient of approximately 1 and a y intercept approximating 0. This was consistent with the similar substitution rates observed between the two regions by Bayesian MCMC analysis (Table 2). Both showed evidence for continuous and discontinuous sequence distributions compared with other subgenogroups. Distributions of pairwise distances between B4 and B5 and between C1 and C2 overlapped, and their similar trajectories to within-subgenogroup (B4 and C1) comparisons demonstrated a process of ongoing divergence without recombination. B4 and B5 indeed retained the same RF group, A, as did C1 and C2 (with RF-W). Comparison of B4 and C1 sequences to other subgenogroups revealed quite distinct relationships. For example, C2 and C4 were similarly divergent from C1 in VP1 (comparing the distributions of yellow and light blue points), but 3Dpol sequences from C4 were substantially divergent (pairwise distance of around 0.4), an observation that can only be accounted for by a recombination event, in this case to RF group L.

Equivalent recombination events are implied by the other intersubgenogroup comparisons comprising B4 (A) to B1 (E), B2 (D), and B3 (G) and C1 (W) to C4 (L), C5 (T), and likely C3 (V) (RF designations in parentheses). Comparison of C1 to C2 and C4 further revealed the separate placement of RF-Y and RF-H, away from the main groups, confirming the occurrence of further spo-

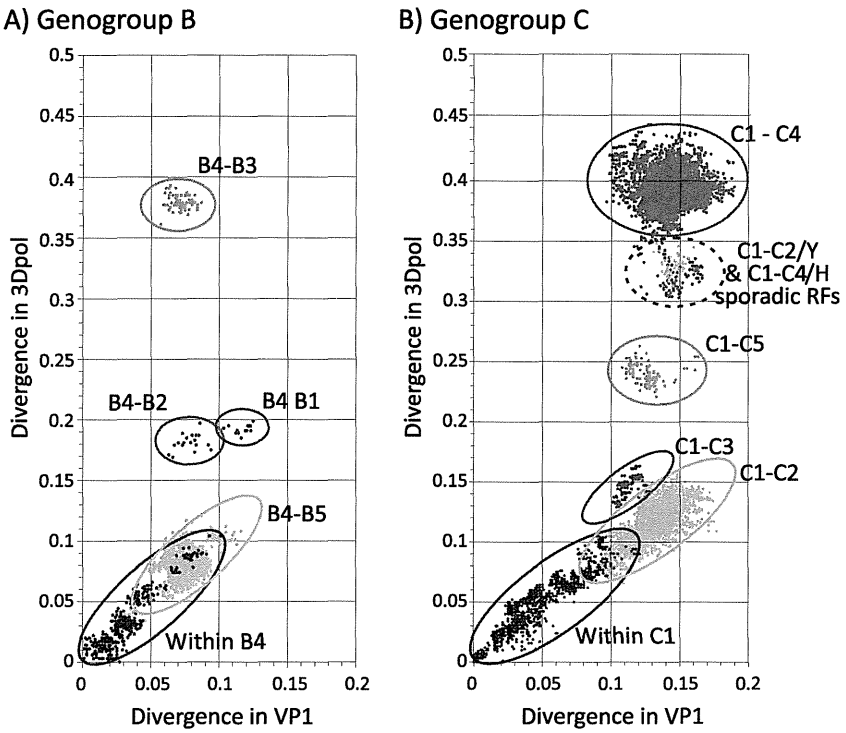

FIG 2 Relationships between sequence divergence (MCL pairwise distances) in the VP1 region (*x* axis) and in 3Dpol (*y* axis) among (A) genogroup B (A) and genogroup C (B) EV71 sequences. In the examples shown, sets of pairwise distances in both regions between GgB4 and C1 to other variants within GgB and GgC are depicted. Note that subgenogroups C2 and C4 both contained within them single sporadic recombinants; these account for the additional groupings of data points encircled by the dotted line.

radic recombination events. Indeed, pairwise comparison of each subgenogroup to each within gB and gC subgroups (30 comparisons [data not shown]) confirmed that only B4/B5 and C1/C2 were consistently equidistant in the two genome regions; these were additionally the only two pairs of subgenogroups that shared the same 3Dpol group (A and W, respectively).

Temporal correlates of recombination in GgB and GgC. To estimate the relationship between virus diversification and the occurrence of recombination in EV71, sequences of each isolate within EV species B and C were compared in the VP1 region to estimate evolutionary divergence and in the 3Dpol region to identify shared or different 3Dpol groupings (Fig. 3). Pairs of isolates with different 3Dpol groups were considered to have undergone recombination. The proportion of isolate comparisons with different 3Dpol groups increased with increasing VP1 divergence in both genogroups B and C (Fig. 3). As previously performed for EV-B serotypes (38), interpolation of the 50% value, combined with the substitution rate for VP1 (Table 2 [7.2×10^{-3} substitutions/site/year]) enabled estimates of approximate half-lives of genogroups B and C EV71 to be made. Values of 0.085 and 0.135 predicted half-lives of 5.9 and 9.4 years for GgB and -C, respectively. This difference is consistent with the observation of lower divergence between recombinant sequences in GgB in the analysis of VP1 and 3Dpol sequences (Fig. 3) and the prolonged existence of subgenogroups C1 and C2, which retained a long-term association with the 3Dpol clade W, despite their substantial sequence divergence in VP1 (pairwise distances ranging from approximately 0.10 to 0.17 [Fig. 2]).

The occurrence of recombination was mapped onto MCMC-generated time-correlated trees (Fig. 4) to estimate when individual recombination events occurred. GgB and GgC displayed different temporal dynamics and patterns of RF succession. For GgB (Fig. 4A), a stepwise, time-related correlation of recombination with VP1 divergence was observed, encompassing isolates collected over a 35-year period. As identified previously, each VP1

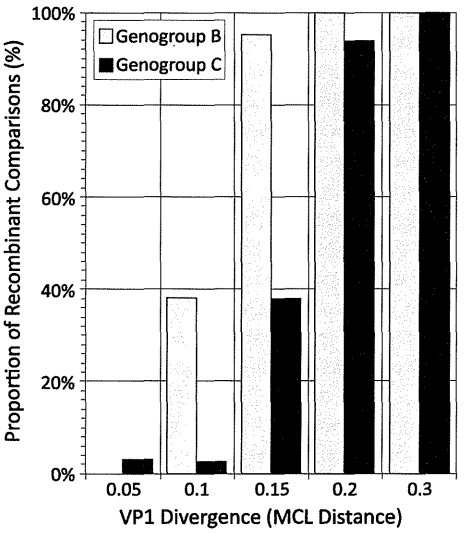

FIG 3 Association between VP1 sequence divergence (the maximum value is shown for each bar on the *x* axis) and the proportion of recombinant comparisons (i.e., belonging to different 3Dpol clades) for GgB and GgC.

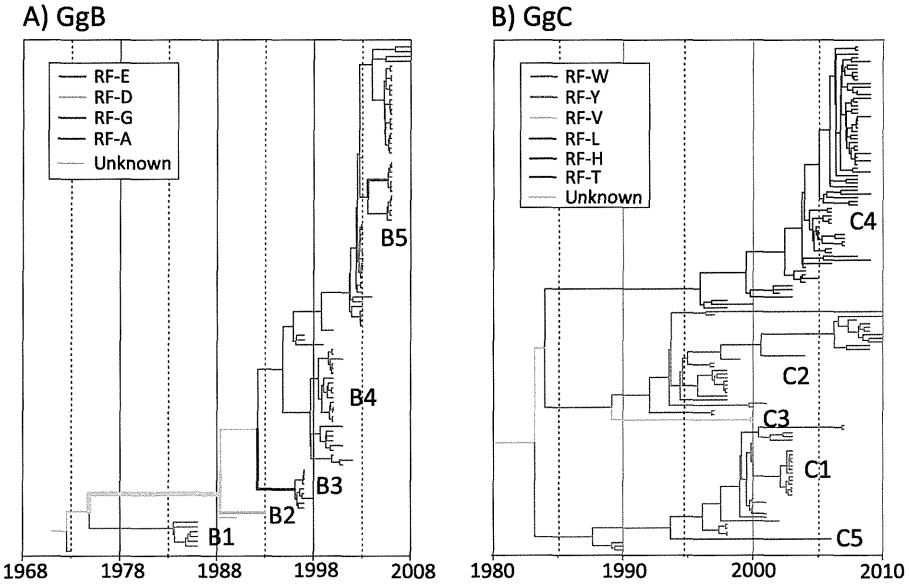

FIG 4 MCMC tree of the VP1 sequences of GgB (A) and GgC (B) from the Asian Pacific region visualized using FigTree and plotted on a temporal *y*-axis scale using their sampling dates. Branches are color coded (see the key in each panel) according to the recombination group of individual sequences and their reconstructed ancestors.

subgenogroup corresponded to a single RF group, with the exception of GgB4 and GgB5 (both RF-A). The consecutive replacements of B1 by B2, B2 by B3, and B3 by B4 each involved viruses bearing distinct 3Dpol region sequences (RF-E to RF-D to RF-G to RF-A). The date of recombination events could be estimated as lying between the MRCA shared by the original RF and the new RF and the isolation date of the first clinical sample with the new RF. Thus, it can be estimated that recombination of the most recent RF group, RF-A, occurred between 1992 and 1997. The subsequent emergence of the associated subgenogroups, GgB4 and GgB5, was characterized by large-scale, short-term outbreaks occurring with a periodicity of approximately 3 years. However, unlike earlier outbreaks (1973 to 1998) involving RF groups E, D, and G, the 3-year spacing of these outbreaks was not immediately preceded by a recombination event even when VP1 divergence was extensive enough to designate a separate subgenogroup (GgB4 and GgB5).

GgC comprised three major lineages that diverged from a common ancestor in 1983 (HPD, 1978 to 1986 [Fig. 4B]). Two of the VP1 lineages in GgC contained one or two sporadic monophyletic RF groups interspersed within one major RF group. It is likely that these sporadic RF groups originated from a single (datable) recombination event, and each were minor and short-lived components of the circulating virus population. The lineage containing GgC1 (RF-W) persisted for at least 17 years (1990 to 2007), and GgC5 (RF-T) emerged as a sporadic RF group in 2006, having undergone a recombination event sometime between 1994 and 2006. The first clinical sample of the second lineage (mainly GgC2, RF-W) was collected in 1997, and this lineage has persisted for 13 years, up to the end of the study period in 2010. This lineage also contained two GgC3 samples belonging to RF-V that were isolated in 2000 and likely recombined between 1989 and 2000. A further sporadic RF group (Y) that appeared in 2010 probably recombined with its unknown second parental strain between 1996 and 2010, exhibiting a long quiescent period before emergence in 2010. The third lineage was comprised entirely of GgC4 sequences, which persisted for 11 years (between 1998 and 2009), displayed time-correlated divergence, and consisted predominantly of RF-L with the exception of two isolates of the sporadic group RF-H (isolated in 2008); this group probably recombined between 2005 and 2008, emerging in 2008 after a short quiescent period. RF-H did not appear to replace the parental RF-L group up to the end of the study in 2010.

DISCUSSION

Detection of recombination in EV71. This study applied methods developed in previous genetic analyses of EV-B viruses to reexamine the occurrence and dynamics of recombination in EV71. EV71 is considered to be the most pathogenic of the currently circulating enteroviruses worldwide, with infections associated with outbreaks of HFMD and serious neurological disease in Southeast Asia. Understanding the underlying interactions between virus evolution and population susceptibility and the biological basis for its severe disease associations are major research priorities, as is the development of preventative or treatment strategies for its control.

In the current study, detection of recombination events was achieved through identification of bootstrap-supported clades by phylogenetic analysis of the 3Dpol region. These groupings were used to categorize EV71 variants into a series of RFs whose assignments were supported by parallel analyses of pairwise distances (see Fig. S2 in the supplemental material); variants within the same RF group showed pairwise distances in the 3Dpol region of <0.19 and of >0.19 between those in different groups. By these criteria, the EV71 3Dpol sequences in this study assembled into 11 clades, and 5 of these clades comprised over 96% of the total nonstructural sequences analyzed. Therefore, the repertoire of 3Dpol RFs was much more restricted in EV71 than that found in species B EVs (37, 38), where 119 E11 variants collected over a 14-year period could be assigned to 43 RF groups, 89 E9 samples into 23

RF groups, and 240 European E30 samples into 26 RF groups. The underlying reasons for this difference in diversity between viruses in EV species A and B are unclear.

Using this classification, comparison of phylogenetic trees from VP1 and 3Dpol regions showed a large number of phylogenetic incongruities indicative of recombination (Fig. 1). Most striking was the interspersed position of 3Dpol sequences from CVA16 variants included in the analysis. As these by definition take an outlier position in the VP1 region, each occurrence therefore represents a recombination event in the evolutionary history of either EV71 or CVA16. Also striking was the difference of tree position of GgB3 and GgC4 in VP1 and in 3Dpol; both grouped away from other members of the same genogroup (10, 17, 24, 66). However, the assertion that these variants show evidence for intertypic recombination, such as GgC4 with CVA16, is not supported by the analysis in the current study. GgC4 variants are, with one exception, assigned to RF-H, a 3Dpol grouping that is distinct from its closest neighbor, RF-L, assigned to CVA16. Although occupying neighboring positions in the tree, their assignment to different RF groups therefore provides evidence against the frequently proposed specific recombination event between GgC4 and CVA16. Subgenogroup B3 showed an analogous change in tree position, as previously described (10), although again without evidence for intertypic recombination, since its 3Dol group (G) is also not shared with any other EV71 or CVA16 variants (Fig. 1) or other EV-A serotype (data not shown).

This tree comparison also revealed the existence of two sporadic recombinants, variants of EV71 with 3Dpol assignments different from the rest of the subgenogroup within which they are classified. These comprise the C2 variant characterized in the current study, JP17/Ac/Y/10, assigned as RF-Y instead of the majority, RF-W (Fig. 1), and the C4 variants CN23/Sz/H/08 and CN19/Bj/H/08, assigned as RF-H instead of RF-L (Fig. 1). The other evident phylogeny violation is the outlier position of the single GgA sequence in VP1 and its inlier position in 3Dpol.

Indeed, rather than representing defined recombination events between serotypes, or indeed recombination between lineages within EV71, the discordant sequence relationships between genome regions in EV71 closely resemble a quite different process of largely independent evolution of genome regions that has been previously observed in species B enteroviruses (32, 37, 38). For echoviruses 9, 11, and 30, evolutionary lineages identified within the capsid region show evidence for recombination with a larger pool of nonstructural region variants that show no systematically closer genetic relationship with one serotype than with any other. In the case of E9, E11, and E30, the 92 RF groups were thus fully interspersed with each other and with 3Dpol groups of other EV-B serotypes, with only very rare occurrences of shared RF groups between different serotypes or indeed lineages within a serotype (37, 38). The observed scattered positions of CVA16 and EV71 3Dpol-associated clades and the lack of shared RF assignments of different subgenogroups observed in the current study are indeed precise mirrors of the pattern observed in EV-B.

Distributions of pairwise distances in the two genome regions (Fig. 2) provided evidence for further recombination events in the evolution of EV71. This analysis method demonstrated abrupt discontinuities in distributions of pairwise distances between the two genome regions, indicative of recombination events accompanying the founding of most subgenogroups within GgB and GgC. This conclusion is consistent with independent evolutionary pathways of structural and nonstructural genome regions identified in EV-B (32). Indeed, only pairwise comparisons between members of the same subgenogroup, or between B1/B2 and C4/C5, showed equality in divergence (i.e., the gradient of the set of pairwise distances approximated unity), which was entailed in their similar substitution rates (Table 2). All other comparisons between subgenogroups revealed disproportionately high and nonlinear greater divergence in the 3Dpol region, indicative of recombination. These plots of pairwise distances help visualize the differing degrees of overall divergence in different genome regions described previously (64) and which are so evident on divergence scans and boot-scanning (10, 17, 24, 66).

Time scale of recombination events. By measuring the relationship between VP1 divergence and occurrence of recombination, as previously carried out for EV-B serotypes (38), it was possible to calculate approximate half-lives for individual RFs of EV71 (Fig. 3). Estimates of 5.9 and 9.4 years for Gg B and GgC overlapped the range observed previously in the EV-B serotypes E9, E30, and E11 (with half-lives of 1.3, 3.1, and 9.8 years, respectively [38]). However, the major EV71 RFs (A, E, G, L, and W) showed decades-long circulation without recombination, a pattern also observed for the E11 RF-DU, which continued to circulate throughout a study period from 1996 to 2008 (38). Variability in recombination frequency is likely shaped by differing viral epidemiologies that govern opportunities for coinfection and generation of hybrid viruses to occur. They may also be influenced by different compatibility restrictions, which would dictate the likelihood of replication-competent viruses being generated by recombination. The marked differences in recombination frequencies observed between human parechovirus (HPeV) type 1 (4 years) and HPeV type 3 (20 years) (7) may indeed be a manifestation of constraints limiting compatibility between viruses with different cell entry mechanisms and, potentially, cellular tropisms (22).

More-precise identification of the individual recombination events in EV71 was achieved through the use of time-correlated trees and superimposition of branching points in the VP1 tree that most parsimoniously accounted for the RF designations in descendant sequences (Fig. 4). These phylogenetic reconstructions for genogroups B and C additionally place recombination events into the differing evolutionary trajectories of GgB and GgC that have been characterized previously (61, 63). GgB is characterized by a series of successive emergence and extinctions of the B1 through B5 subgenogroups over the period from 1970 to the present day, with outbreaks occurring throughout South and East Asia in a cycle of approximately every 3 years (1993, 1997, 2000, 2003, 2006, and 2008) (9, 23, 46, 58, 62). The association between the founding of each lineage and recombination is clearly evident from the phylogenetic analysis. This provides the means to estimate dates within fairly narrow windows for their occurrence. These tree-based estimates are consistent with the TMRCA estimates from diversity/substitution rate calculations in both the VP1 and 3Dpol regions (Table 2) (61).

In contrast, it has been established that different subgenogroups of GgC EV71 variants have coexisted for at least 25 years, with three separate lineages (C1, C2, and C5) emerging in the 1980s and continuing to circulate to the present (5, 58, 61). This contrasting pattern is exemplified in a previous characterization of isolates of EV71 in Malaysia; GgB variants were isolated only during periodic major outbreaks, whereas GgC isolates were de-